Original Article

Concurrent brain structural and functional alterations in patients with chronic unilateral vestibulopathy

Lihong Si[1], Bin Cui[1], Zheyuan Li[1], Xiang Li[2], Kangzhi Li[1], Xia Ling[1], Bo Shen[2], Xu Yang[1]

[1]Department of Neurology, Aerospace Center Hospital (Peking University Aerospace School of Clinical Medicine), Beijing, China; [2]The First Affiliated Hospital of Jinzhou Medical University, Jinzhou, China

Contributions: (I) Conception and design: X Yang; (II) Administrative support: X Yang; (III) Provision of study materials or patients: L Si; (IV) Collection and assembly of data: L Si, B Cui, Z Li, X Li, K Li, X Ling, B Shen; (V) Data analysis and interpretation: L Si, B Cui, X Yang; (VI) Manuscript writing: All authors; (VII) Final approval of manuscript: All authors.

Correspondence to: Xu Yang. Department of Neurology, Aerospace Center Hospital (Peking University Aerospace School of Clinical Medicine), 15 Yuquan Road, Beijing 100049, China. Email: yangxu2011@163.com.

Background: Chronic unilateral vestibulopathy (CUVP) is a common chronic vestibular syndrome which may be caused by incomplete vestibular dynamic compensation. Neuroimaging technology provides important clues to explore the mechanism of complicated by vestibular dynamic compensation in patients with CUVP. However, previous studies mostly used positron emission tomography (PET) and functional magnetic resonance imaging (fMRI) to investigate the changes of brain function in these patients during the task state, few studies have investigated the alterations during the resting state, Therefore, the study aimed to investigate the possible brain structural and functional alterations in patients with CUVP and explore the dynamic compensation state in patients with CUVP.

Methods: We recruited 18 patients with right CUVP and 18 age-, gender-, and education level-matched healthy controls (HCs). Vestibular evaluations, such as videonystagmography and caloric tests, were performed. All participants underwent Dizziness Handicap Inventory (DHI) assessment. All participants underwent multimodal magnetic resonance imaging of the brain, including fMRI and three-dimensional T1-weighted MRI. We analyzed the amplitude of low frequency fluctuations (ALFF), regional homogeneity (ReHo), seed based functional connectivity, and voxel-based morphometry (VBM).

Results: Compared with HCs, CUVP patients showed significantly increased ALFF values in the right supplementary motor area, significantly decreased ALFF values in the right middle occipital gyrus, significantly decreased ReHo values in the bilateral superior parietal lobule, and significantly enhanced ReHo values in the bilateral cerebellar hemisphere [both $P<0.05$, family-wise error (FWE) corrected]. Compared with HCs, patients with CUVP showed increased gray matter volumes in the left medial superior frontal gyrus and left middle cingulate gyrus [$P<0.001$, false discovery rate (FDR) corrected]. Compared with HCs, in patients with CUVP, functional connectivity was enhanced between the left medial superior frontal gyrus and the left orbital inferior frontal gyrus and left angular gyrus and was significantly decreased between the left medial superior frontal gyrus and the right dorsolateral superior frontal gyrus (both $P<0.01$, FWE corrected). Pearson correlation analysis showed that there was a positive correlation between DHI score and VBM value of the left medial superior frontal gyrus in patients with CUVP ($r=-0.430$, $P=0.003$).

Conclusions: This study identified abnormalities of neuronal activity intensity and overall activity synchronization in multiple brain regions in patients with CUVP, suggesting that patients with CUVP have extensive brain functional abnormalities, which in turn affects their spatial perception and motor perception. Increased gray matter volume and functional connectivity of the default mode network may be used as potential imaging biomarkers of chronic symptoms in patients with CUVP.

Keywords: Chronic unilateral vestibulopathy (CUVP); resting state-functional magnetic resonance imaging amplitude of low frequency fluctuation; gray matter volume; functional connectivity

Submitted Jun 22, 2021. Accepted for publication Mar 02, 2022.
doi: 10.21037/qims-21-655
View this article at: https://dx.doi.org/10.21037/qims-21-655

Introduction

Chronic unilateral vestibulopathy (CUVP) is a common chronic vestibular syndrome. Patients with CUVP usually present with persistent dizziness and postural instability (1-4). Vestibular function is highly dependent on the integration of a variety of sensory organs that process visual, proprioceptive, and tactile information (5). Interaction between different senses enables the possibility of sensory substitution in unilateral vestibulopathy (UVP) (6-8). Studies have shown that chronic symptoms of CUVP may be related to incomplete vestibular compensation, psychological factors, and reliance on visual information (9). Our previous study found that there was no significant correlation between canal paresis (CP) value or course of disease in patients with CUVP or a patient's Dizziness Handicap Inventory (DHI) score and subscores. This suggests that residual peripheral vestibular insufficiency in patients with CUVP may not be the only factor that impacts their chronicity. Rather, CUVP may also be caused by incomplete vestibular dynamic compensation and failure to restore higher-order perceptual function. These factors can produce subjective feelings such as vertigo and instability in patients during prolonged physical exertion (10).

In recent years, neuroimaging technology has been used extensively in multi-disciplinary research fields and provides important clues to explore the mechanism of vestibular compensation in patients with UVP (11). Positron emission tomography (PET) studies of patients with acute unilateral vestibulopathy (AUVP) have shown that their cortical activation patterns resemble those observed in healthy participants during unilateral vestibular caloric stimulation. In these patients, the parieto-insular vestibular cortex (PIVC), posterior insular cortex, posterolateral thalamus, anterior cingulate gyrus, and hippocampus were significantly activated, while the visual and somatosensory cortex and part of the auditory cortex were deactivated (12-14). Researchers have speculated that the asymmetric activation of the PIVC area of the posterior insular cortex may be due to the high resting discharge rate of the contralateral vestibular nucleus, which suggests that the vestibular system, visual system, and somatosensory system work together to maintain body balance (15,16), and the interaction of different senses to maintain balance provides the possibility for sensory substitution (17). Helmchen *et al*. (18) performed a functional magnetic resonance imaging (fMRI) study of patients with vestibular neuritis based on the independent component analysis (ICA). The results demonstrated reduced functional connectivity (FC) in the intraparietal sulcus (IPS) near the supramarginal gyrus on the contralateral side of the lesion during the acute stage of vestibular neuritis. When vestibular function recovered, the IPS, an area which is involved in spatial orientation and multisensory integration, exhibited increased FC over time, suggesting that it was the consequence of central compensation.

Most previous studies have used PET and fMRI to investigate the changes of brain function in patients with UVP during the task state, but few studies have investigated the alterations in FC during the resting state, and most studies have focused on patients with AUVP. The wide application of voxel-based morphometry (VBM) and fMRI in clinics provides new research approaches to explore the compensatory state of the vestibular center in patients with CUVP based on structural and functional alterations of the brain. This study investigated the functional and structural alterations in patients with CUVP by using the multimodal imaging techniques of amplitude of low frequency fluctuation (ALFF), regional homogeneity (ReHo), and VBM. We hoped to provide a deeper understanding of the central compensation state of patients with CUVP and provide a scientific basis to guide vestibular rehabilitation in patients with CUVP. We present the following article in accordance with the Materials Design Analysis Reporting (MDAR) reporting checklist (available at https://qims.amegroups.com/article/view/10.21037/qims-21-655/rc).

Methods

Participants

The patients and healthy controls (HCs) analyzed in this study

were the same as those included in our previous study (10). A total of 18 right-sided CUVP patients who were admitted to Aerospace Center Hospital from September 2018 to September 2019 were included, including 6 males and 12 females, with an average age of 47.94±11.01 years (range, 17 to 65 years). The median duration of disease was 10 months (interquartile range, 12 months). A total of 18 age- and gender-matched HCs were included.

Vestibular function examination and routine brain MRI were performed on all participants. According to the bithermal caloric test, UVP refers to patients with an asymmetric vestibular response >25% (i.e., CP >25%) that was calculated using Jongkees' formula. A patient was considered to exhibit the acute phase of UVP if the symptom duration was less than 2 weeks. If the symptom duration was between 2 weeks and 3 months, the patient was considered to be in the subacute phase, and if symptoms lasted for more than 3 months, the patient was considered to be in the chronic phase. In this study, the duration of disease in all patients with CUVP was ≥3 months. All patients were evaluated based on the DHI. Then, all participants were further scanned with fMRI.

The study was conducted in accordance with the Declaration of Helsinki (as revised in 2013) and approved by the Ethics Committee of Aerospace Center Hospital (Peking University Aerospace School of Clinical Medicine) (No. 20180314-ST-04). Written informed consent was provided by each participant prior to the study.

MRI data acquisition

This study used a 3.0-Tesla MR scanner (MAGNETOM Skyra syngo MR D13; Siemens, Erlangen, Germany) with a 32-channel combined head and neck coil for data acquisition. During the image acquisition, the participant's head was immobilized to avoid head movement. Participants were instructed to relax with their eyes closed but remained awake throughout the scan. The anatomical images were acquired using a 3-dimensional (3D) magnetization-prepared rapid gradient-echo (MP-RAGE) sequence, 192 slices in total, repetition time (TR)/echo time (TE)/flip angle (FA) =1,900 ms/2.43 ms/8°, field of view (FOV) =256×256×256 mm^3, and voxel size =1.0×1.0×1.0 mm^3. The resting-state functional images were recorded using an echo-planar imaging sequence, 200 volumes in total, TR/TE/FA=2,000 ms/30 ms/90°, FOV =222×222×222 mm^3, voxel size =3.0×3.0×3.0 mm^3, and scanning time =6 minutes and 48 seconds.

fMRI data analysis

We performed fMRI data preprocessing using Data Processing Assistant for Resting-State fMRI Analysis (DPARSFA) software based on MATLAB 2013 platform (19). Image data was converted from digital imaging and communications in medicine (DICOM) format to Neuroimaging Informatics Technology Initiative (NIfTI) using Statistical Parametric Mapping (SPM) 12 (https://www.fil.ion.ucl.ac.uk/spm/). The first 10 time points were removed to avoid instability. The 35th slice was taken as the reference slice. Data with a head 3D translation exceeding 1.5 mm and/or 3D rotation exceeding 1.5° were excluded. Linear drift of the blood-oxygen-level-dependent (BOLD) signal due to machine heating during scanning was removed. The interference signal in BOLD signal was removed using a linear regression model. The local spatial data of different participants was aligned to the same standard space to resolve the difference in brain morphology between different participants and the inconsistency of spatial positions during scanning. The voxel size was sampled to 3 mm × 3 mm × 3 mm, and the registration method was diffeomorphic anatomical registration using exponentiated lie algebra (DARTEL). To reduce registration errors and increase the normality of the data, data was smoothed at a Gaussian smoothing kernel [full width at half maximum (FWHM)] of 8 mm × 8 mm × 8 mm.

ALFF

To analyze ALFF, the pre-processed fMRI data were processed using DPARSFA. The time series of a given voxel in the brain was transformed to the frequency domain through a fast Fourier transform to obtain the corresponding power spectrum. The average square root of the power spectrum across 0.01–0.08 Hz was calculated as the ALFF value. After calculating the ALFF value of all voxels across the whole brain, a whole brain map of ALFF values for each participant was obtained. Each individual's ALFF value was then transformed to a Z-score to avoid individual differences among participants. It was still necessary to z-normalize each individual's ALFF value to avoid individual differences among participants. A 2-sample *t*-test was applied to analyze differences in ALFF between CUVP patients and HCs with age and gender used as covariates.

ReHo

The pre-processed fMRI data were processed using the

DPARSFA to analyze ReHo. We generated Reho maps by calculating Kendall's coefficient concordance (KCC) for a given voxel's time series with its nearest neighbors (26 voxels) on a voxel-wise basis. The data were then smoothed using a Gaussian filter with 8-mm FWHM to reduce noise and residual differences in gyrus anatomy. The ReHo maps were generated for each participant in each group. Differences in ReHo between CUVP patients and HCs were analyzed using a 2-sample *t*-test, with age and gender used as covariates. Statistical analysis was performed using correction for family-wise error (FWE), and the significance of group differences was set at P<0.05.

VBM

Based on MATLAB 2013 (MathWorks, Natick, MA, USA), the 3D brain structural image was processed with SPM8. Pre-processing of structural images for VBM analyses was performed using SPM12 and the CAT12 toolbox. The original image was registered, segmented, and smoothed (6-mm full width at half height Gaussian kernel). A 2-sample *t*-test was used to compare the differences in gray matter (GM) volume between CUVP patients and HCs. Participant age and gender were used as covariates, and the statistical threshold was P<0.05 [false discovery rate (FDR) correction]. Pearson's correlation analysis was performed to analyze the correlation between with VBM alterations and DHI total score in patients with CUVP. Statistical significance was set at P<0.05 using FWE correction.

FC

Using DPARSFA software, the brain regions with different GM volumes were taken as regions of interest (ROIs) to analyze the FC. The differences in FC between the CUVP group and HCs were compared with a 2-sample *t*-test, with age and gender included as additional covariates, and analyzed with the random effects model. Statistical significance was set at P<0.05 using FWE correction during analysis.

Results

ALFF

Compared with HCs, the ALFF value in the right supplementary motor area (SMA) was significantly higher in CUVP patients (X=9; Y=3; Z=54; K=66). However, the ALFF value in the right middle occipital gyrus (X=30; Y=−84; Z=3; K=87) was significantly lower in patients with CUVP than in HCs (P=0.035, FWE corrected) (*Figures 1*,*2*).

ReHo

Compared with HCs, the ReHo values in the left superior parietal lobule (X=−24; Y=−42; Z=63; K=100) and the right superior parietal lobule (X=18; Y=−54; Z=69; K=139) were significantly decreased in patients with CUVP (P<0.01, FWE corrected). However, the ReHo values in the left cerebellar hemisphere (X=−18; Y=−81; Z=45; K=177) and the right cerebellar hemisphere (X=45; Y=−78; Z=−24; K=97) were significantly enhanced in patients with CUVP compared with HCs (P=0.02, FWE corrected, *Figures 3*,*4*).

VBM

Compared with HCs, the GM volume in the left medial superior frontal gyrus (X=−16.5; Y =46.5; Z=52.5; K=326) and the left middle cingulate gyrus (X=−7.5; Y=−16.5; Z=34.5) was significantly higher in patients with CUVP (P<0.001, FDR corrected; *Figure 5*).

Seed-based FC

Compared with HCs, patients with CUVP demonstrated enhanced FC between the left medial superior frontal gyrus and the left orbital inferior frontal gyrus, left angular gyrus, and weakened FC between the left medial superior frontal gyrus and the right dorsolateral superior frontal gyrus (P<0.01, FWE corrected; *Figure 6*).

Correlation analysis

There was a positive correlation between DHI score and VBM value of the left medial superior frontal gyrus in patients with CUVP (r=−0.430, P=0.003).

Discussion

In this study, the areas with decreased ALFF values mainly reflected the brain areas related to the visual cortex, suggesting that the activity of visual cortical neurons and cortical excitability decreased in patients with CUVP. Consistent with our previous study, intra-network FC analysis showed decreased FC in the right middle occipital gyrus within lateral visual network in CUVP patients (10).

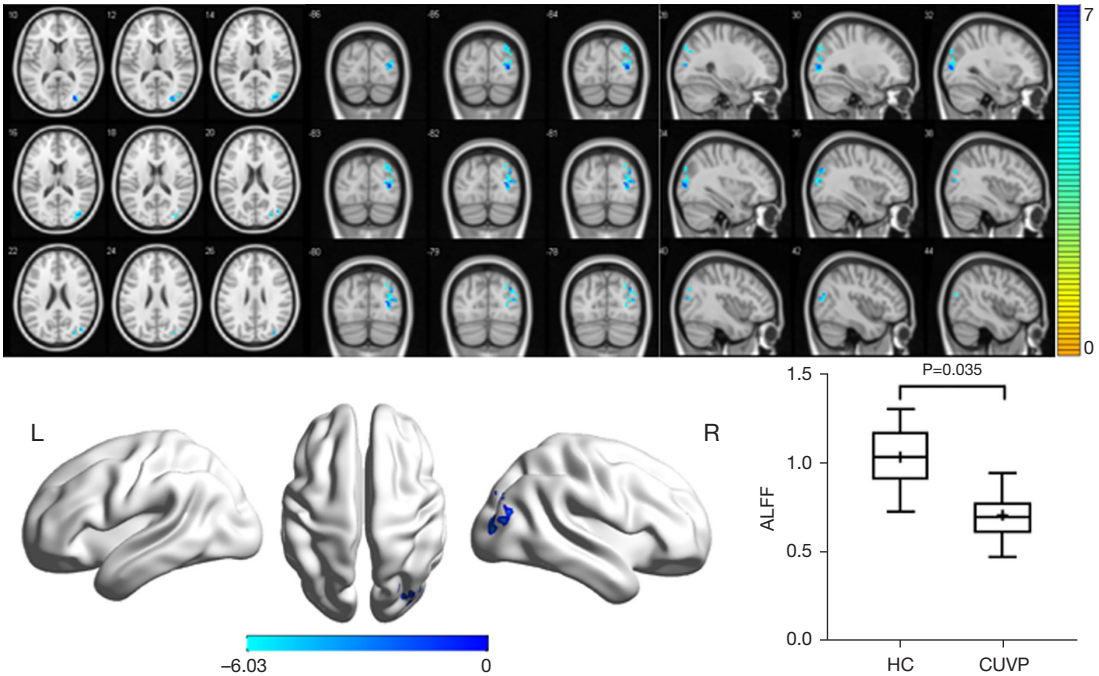

Figure 1 ALFF values in the right middle occipital gyrus were significantly lower in patients with CUVP than in HCs (X=30; Y=−84; Z=3; P=0.035, FWE corrected). X, Y, Z: MNI coordinate. ALFF, amplitude of low frequency fluctuation; CUVP, chronic unilateral vestibulopathy; FWE, family-wise error; HCs, healthy controls; L, left; MNI, Montreal Neurological Institute; R, right.

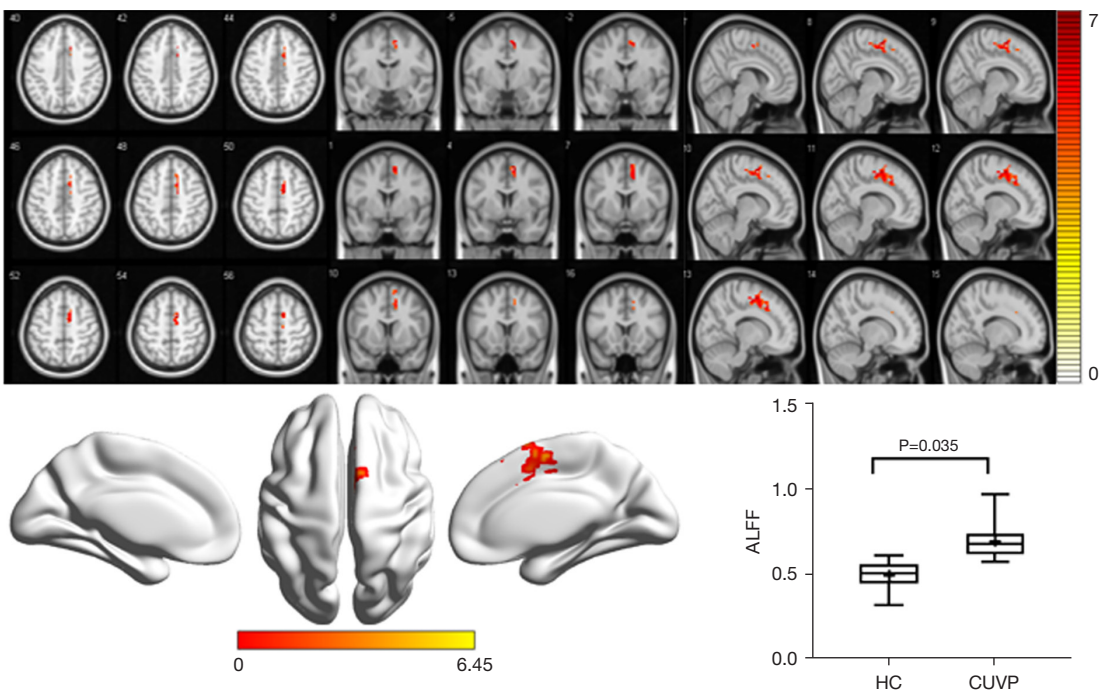

Figure 2 ALFF values in the right supplementary motor area were significantly higher in patients with CUVP (X=9; Y=3; Z=54; P=0.035; FWE corrected) than in HCs. X, Y, Z: MNI coordinate. ALFF, amplitude of low frequency fluctuation; CUVP, chronic unilateral vestibulopathy; FWE, family-wise error; HCs, healthy controls; MNI, Montreal Neurological Institute.

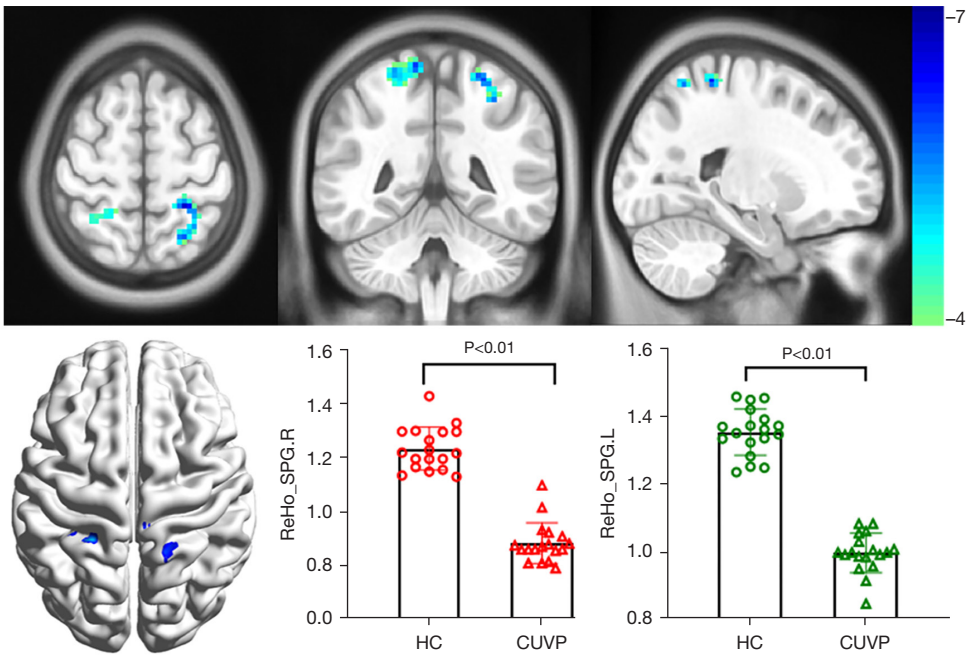

Figure 3 The ReHo values in the left superior parietal lobule (X=−24; Y=−42; Z=63; K=100) and right superior parietal lobule (X=18; Y=−54; Z=69; K=139) were significantly lower in patients with CUVP than in HCs (P<0.01, FWE corrected). X, Y, Z: MNI coordinate; K: cluster size. CUVP, chronic unilateral vestibulopathy; FWE, family-wise error; HCs, healthy controls; MNI, Montreal Neurological Institute; ReHo, regional homogeneity; SPG.R, right superior parietal lobule; SPG.L, left superior parietal lobule.

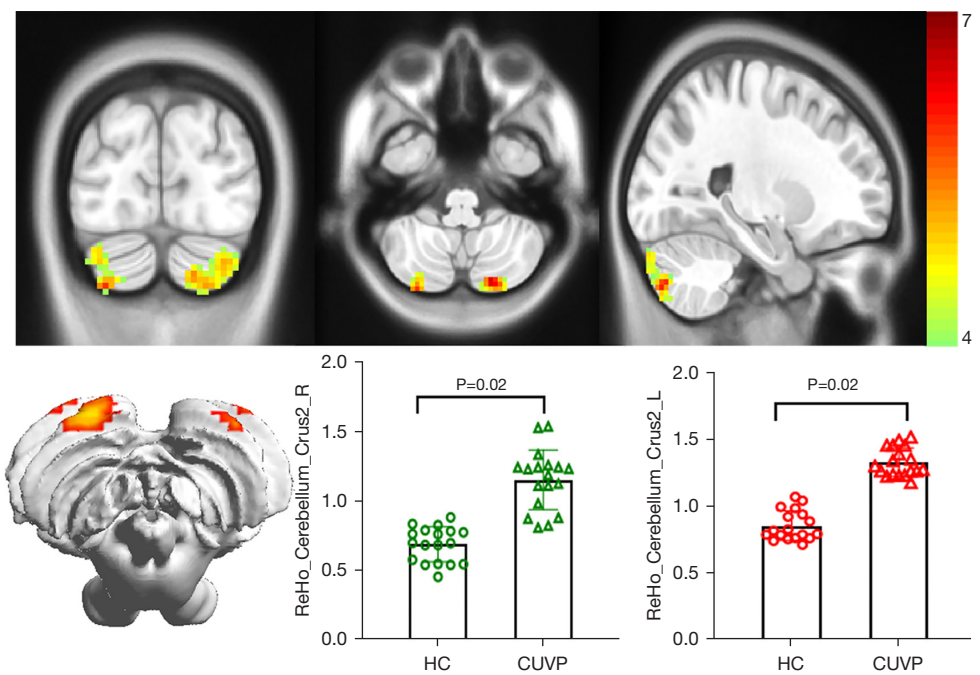

Figure 4 The ReHo values in the lower part of the left cerebellar hemisphere (X=−18; Y=−81; Z=45; K=177) and the lower part of the right cerebellar hemisphere (X=45; Y=−78; Z=24; K=97) were significantly higher in patients with CUVP than in HCs (P=0.02, FWE corrected). X, Y, Z: MNI coordinate; K: cluster size. CUVP, chronic unilateral vestibulopathy; FWE, family-wise error; HCs, healthy controls; MNI, Montreal Neurological Institute; ReHo, regional homogeneity.

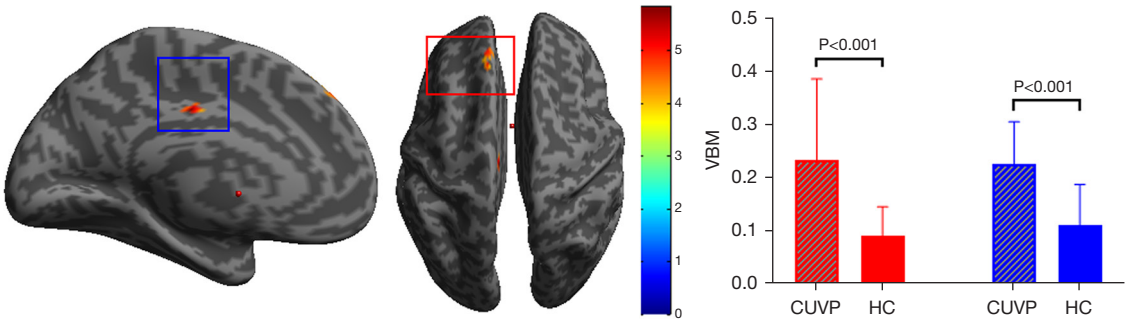

Figure 5 The GM volume in the left medial superior frontal gyrus (X=−16.5; Y=46.5; Z=52.5; K=326) and left middle cingulate (X=−7.5; Y=−16.5; Z=34.5) gyrus was significantly higher in patients with CUVP than in HCs (P<0.001, FDR corrected). X, Y, Z: MNI coordinate; K: cluster size. GM, gray matter; CUVP, chronic unilateral vestibulopathy; FDR, false discovery rate; HCs, healthy controls; MNI, Montreal Neurological Institute; VBM, voxel-based morphometry.

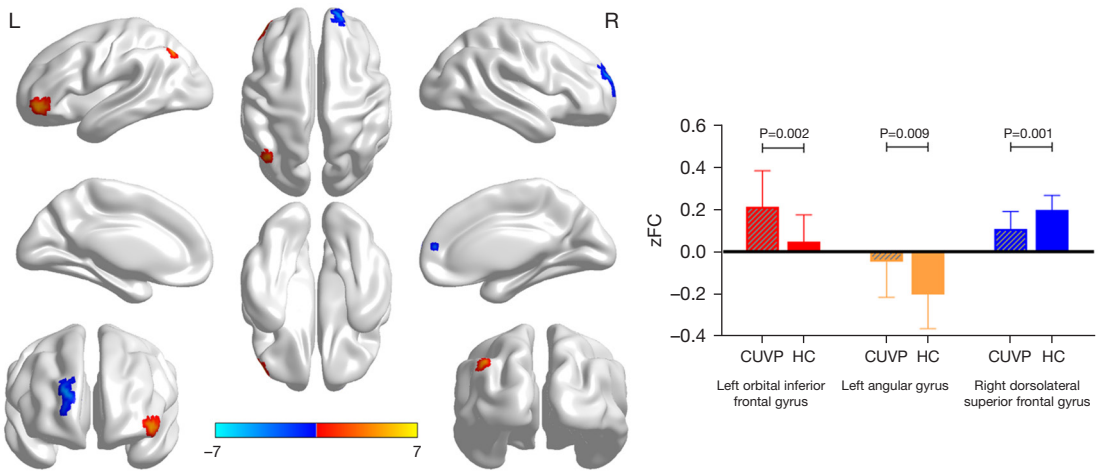

Figure 6 Compared with HCs, patients with CUVP demonstrated enhanced FC between the left medial superior frontal gyrus and the left orbital inferior frontal gyrus, the left angular gyrus, and weakened FC between the left medial superior frontal gyrus and the right dorsolateral superior frontal gyrus (P<0.01, FWE corrected). CUVP, chronic unilateral vestibulopathy; FC, functional connectivity; FWE, family-wise error; GM, gray matter; HCs, healthy controls; L, left; R, right; zFC, z-score of functional connectivity value.

Maintaining the balance of the human body and its relationship with the environment requires input from vision, vestibular perception, and the proprioceptive system, and is further coordinated by the integration of the central nervous system. The relative weights of these 3 systems are constantly adjusted to maintain human balance and accurately perceive the latitudinal position and ensure the balance of clear and stable vision, posture, and various movements. This is the physiological basis of the sensory substitution mechanism of dynamic compensation in patients with UVP. When the vestibular information conflicts with visual information, the body will prioritize activating the vestibular cortex to deal with the conflicting sensory information input, especially in daily high-frequency exercise (20). Cousins *et al.* (6) suggested that the weight of visual information increased in patients with UVP during the dynamic compensatory period, which is an adaptive mechanism against the lack of vestibular information and suggests the occurrence of visual substitution. Deutschländer *et al.* (21) applied visual stimulation to 14 patients with CUVP that was caused by acoustic neuroma resection. The fMRI findings showed that activation of the visual cortex was

weakened in patients with CUVP relative to that of HCs. The authors believed that the decreased response to visual stimulation in patients with CUVP was related to the reduction of oscillopsia.

Based on the further analysis of the 18 CUVP patients included in this study, we speculate that severe vertigo, instability, and other symptoms of the acute phase of CUVP prevented patients from undergoing prompt vestibular rehabilitation treatment. These patients actively avoided visual stimuli, which led to poor visual substitution and resulted in chronic dizziness and instability. These symptoms were aggravated during quick head turns and fast movements. In this study, the areas with increased ALFF values in patients with CUVP were mainly in the brain areas related to the sensorimotor network, especially in the SMA, which contributes to many aspects of motion control (22). SMA is related to postural regulation and proximal limb movement and plays a major role in advanced motor regulation (22). The increased spontaneous brain activity of the sensorimotor network may be the manifestation of behavior substitution in patients with CUVP (i.e., impaired vestibular sensation and poor visual substitution). These patients rely more on strengthening their body posture control and vestibular compensation, but this reliance can lead to the development of risky posture control strategies and a sense of instability.

In this study, we found that the ReHo values in the bilateral superior parietal lobule were decreased significantly in patients with CUVP, indicating that the spontaneous activity in the bilateral superior parietal lobule was altered in patients with CUVP. The posterior parietal cortex is associated with body localization and functional integration and involved in dorsolateral vestibule and motor control information flow (13,23-29). Cornette *et al*. (30) found that the posterior parietal cortex (BA7) is involved in visual-spatial information processing. Naito *et al*. (13) found that the posterior parietal cortex is involved in the integration of multiple sensory inputs related to perceptual spatial movement and direction, which is very important for 3D coding (31-33). These findings suggest that the abnormal spontaneous activity in the bilateral vestibular cortex in patients with CUVP may lead to abnormal integration of sensory information, which may be related to chronic dizziness. In this study, we also found a significant increase in ReHo values in the lower part of the left cerebellar hemisphere, the right cerebellar hemisphere, and the lower cerebellar hemisphere in patients with CUVP. The integration of proprioceptive information with motor vestibular function in the lower part of the cerebellum is closely related to the maintenance of body balance and posture, therefore this may be a compensatory strategy for patients with CUVP. Poor processing of motor visual information in patients with CUVP leads to increased reliance on strengthening body posture control to maintain balance.

Based on VBM analysis, we found that GM volume in the left middle cingulate gyrus and the left medial superior frontal gyrus was increased in patients with CUVP. The middle cingulate gyrus participates in the processes of emotion, pain, and cognitive control. The medial superior frontal gyrus is the core area of the default mode network (DMN) (34) and is activated to participate in many memory-related cognitive and motor control tasks, as well as self-related processing (such as self-assessment and self-decision-making), which is the central system of the DMN (22,35), and the main neural basis of self or self-related processing (36-39). The DMN is the most significant brain network during the resting state; it participates in the monitoring of the internal and external environment and the processing of emotion and cognition. The DMN includes the medial prefrontal cortex, posterior cingulate cortex, anterior cingulate lobe, bilateral inferior parietal lobule, and medial temporal lobe. The anterior medial subarea of the superior frontal gyrus has anatomical connections with the cingulate cortex (mainly with the anterior cingulate cortex and middle cingulate cortex), but has a positive functional connection with the middle cingulate cortex and DMN, which is related to the cognitive control process (40-42). In this study, patients with CUVP demonstrated enhanced FC between the left middle frontal gyrus and left orbital inferior frontal gyrus and left angular gyrus, as well as weakened FC between the right dorsolateral superior frontal gyrus. Enhanced FC was mainly concentrated in the DMN. An fMRI study of patients with AUVP conducted by Klingner *et al*. (43) showed that the functional activity of DMN was increased and the FC between DMN and other networks, such as the somatosensory cortex, auditory, vestibular, insular cortex, motor cortex, and occipital cortex, was decreased. With the recovery of peripheral vestibular function, the FC returned to normal. The authors believe that it is a compensatory strategy for the body in the acute stage of UVP, even when in the resting state. In patients with AUVP, persistent vertigo is caused by spontaneous nystagmus because the body needs to deal with the increased demand for the task network due to multiple sensory afferent conflicts. In this study, the FC of DMN in

patients with CUVP was enhanced, which may have been the result of long-term adaptation of the body. while the further enhanced task was for the network to obtain the surrounding spatial environment and its own positioning information, and then contribute to the occurrence of chronic symptoms in patients with CUVP.

Patients with chronic dizziness are more likely to have anxiety or depressive disorders, which seriously affect their quality of life. In this study, we used DHI to assess functional, physical, and emotional conditions of patients and analyzed the correlation between DHI score and alterations in brain function. Our findings showed a positive correlation between DHI score and VBM value of the left medial superior frontal gyrus in patients with CUVP. Previous studies (44-46) have found a significantly moderate positive correlation between the DHI and hospital anxiety and depression scale (HADS) scores in patients with dizziness. However, further studies are also needed to screen patients for symptoms of anxiety and depression using psychometric scales, such as HADS and Zung's self-rating anxiety/depression scale (SAS) to further explore the relationship between anxiety/depression and brain functional alterations in patients with CUVP.

Limitations

This study had several limitations. First, the relatively small sample size may have limited our ability to detect more alterations in CUVP patients, as well as perform a correlation analysis. Second, although all patients in this study were in the chronic stage, their etiology and course of disease differed, and their compensation strategies varied. Therefore, it is necessary to make a further stratified analysis in patients with CUVP with different etiology and course of disease to explore the differences in brain functional changes and further understand the main causes of chronicity.

Conclusions

This study found abnormalities of neuronal activity intensity and overall activity synchronization in multiple brain regions in patients with CUVP, suggesting that patients with CUVP have extensive brain functional abnormalities. The increased GM volume and enhanced FC of DMN may be used as potential imaging biomarkers for chronic symptoms in patients with CUVP.

Acknowledgments

Funding: The study was supported by Aerospace Center Hospital (No. YN201802).

Footnote

Reporting Checklist: The authors have completed the MDAR reporting checklist. Available at https://qims.amegroups.com/article/view/10.21037/qims-21-655/rc

Conflicts of Interest: All authors have completed the ICMJE uniform disclosure form (available at https://qims.amegroups.com/article/view/10.21037/qims-21-655/coif). The authors have no conflicts of interest to declare.

Ethical Statement: The authors are accountable for all aspects of the work in ensuring that questions related to the accuracy or integrity of any part of the work are appropriately investigated and resolved. The study was conducted in accordance with the Declaration of Helsinki (as revised in 2013). This study was approved by the Ethics Committee of Aerospace Center Hospital (Peking University Aerospace School of Clinical Medicine) (No. 20180314-ST-04), and informed consent was provided by all individual participants.

References

1. Kerber KA. Acute Vestibular Syndrome. Semin Neurol 2020;40:59-66.
2. Lacour M, Helmchen C, Vidal PP. Vestibular compensation: the neuro-otologist's best friend. J Neurol 2016;263 Suppl 1:S54-64.
3. Welgampola MS, Bradshaw AP, Halmagyi GM. Assessment of the Vestibular System: History and Physical Examination. Adv Otorhinolaryngol 2019;82:1-11.

4. Sadeghi NG, Sabetazad B, Rassaian N, Sadeghi SG. Rebalancing the Vestibular System by Unidirectional Rotations in Patients With Chronic Vestibular Dysfunction. Front Neurol 2019;9:1196.
5. Angelaki DE, Cullen KE. Vestibular system: the many facets of a multimodal sense. Annu Rev Neurosci 2008;31:125-50.
6. Cousins S, Cutfield NJ, Kaski D, Palla A, Seemungal BM, Golding JF, Staab JP, Bronstein AM. Visual dependency and dizziness after vestibular neuritis. PLoS One 2014;9:e105426.
7. Horak FB, Nashner LM, Diener HC. Postural strategies associated with somatosensory and vestibular loss. Exp Brain Res 1990;82:167-77.
8. Lacour M, Barthelemy J, Borel L, Magnan J, Xerri C, Chays A, Ouaknine M. Sensory strategies in human postural control before and after unilateral vestibular neurotomy. Exp Brain Res 1997;115:300-10.
9. Panichi R, Faralli M, Bruni R, Kiriakarely A, Occhigrossi C, Ferraresi A, Bronstein AM, Pettorossi VE. Asymmetric vestibular stimulation reveals persistent disruption of motion perception in unilateral vestibular lesions. J Neurophysiol 2017;118:2819-32.
10. Si L, Cui B, Li Z, Li X, Li K, Ling X, Shen B, Yang X. Altered Resting-State Intranetwork and Internetwork Functional Connectivity in Patients With Chronic Unilateral Vestibulopathy. J Magn Reson Imaging 2021. [Epub ahead of print]. doi: 10.1002/jmri.28031.
11. Baier B, Müller N, Rhode F, Dieterich M. Vestibular compensation in cerebellar stroke patients. Eur J Neurol 2015;22:416-8.
12. Stephan T, Deutschländer A, Nolte A, Schneider E, Wiesmann M, Brandt T, Dieterich M. Functional MRI of galvanic vestibular stimulation with alternating currents at different frequencies. Neuroimage 2005;26:721-32.
13. Naito Y, Tateya I, Hirano S, Inoue M, Funabiki K, Toyoda H, Ueno M, Ishizu K, Nagahama Y, Fukuyama H, Ito J. Cortical correlates of vestibulo-ocular reflex modulation: a PET study. Brain 2003;126:1562-78.
14. Bense S, Stephan T, Yousry TA, Brandt T, Dieterich M. Multisensory cortical signal increases and decreases during vestibular galvanic stimulation (fMRI). J Neurophysiol 2001;85:886-99.
15. Alessandrini M, Pagani M, Napolitano B, Micarelli A, Candidi M, Bruno E, Chiaravalloti A, Di Pietro B, Schillaci O. Early and phasic cortical metabolic changes in vestibular neuritis onset. PLoS One 2013;8:e57596.
16. Bense S, Bartenstein P, Lochmann M, Schlindwein P, Brandt T, Dieterich M. Metabolic changes in vestibular and visual cortices in acute vestibular neuritis. Ann Neurol 2004;56:624-30.
17. Suh MW, Lee HJ, Kim JS, Chung CK, Oh SH. Speech experience shapes the speechreading network and subsequent deafness facilitates it. Brain 2009;132:2761-71.
18. Helmchen C, Ye Z, Sprenger A, Münte TF. Changes in resting-state fMRI in vestibular neuritis. Brain Struct Funct 2014;219:1889-900.
19. Chao-Gan Y, Yu-Feng Z. DPARSF: A MATLAB Toolbox for "Pipeline" Data Analysis of Resting-State fMRI. Front Syst Neurosci 2010;4:13.
20. Roberts RE, Ahmad H, Arshad Q, Patel M, Dima D, Leech R, Seemungal BM, Sharp DJ, Bronstein AM. Functional neuroimaging of visuo-vestibular interaction. Brain Struct Funct 2017;222:2329-43.
21. Deutschländer A, Hüfner K, Kalla R, Stephan T, Dera T, Glasauer S, Wiesmann M, Strupp M, Brandt T. Unilateral vestibular failure suppresses cortical visual motion processing. Brain 2008;131:1025-34.
22. Nachev P, Kennard C, Husain M. Functional role of the supplementary and pre-supplementary motor areas. Nat Rev Neurosci 2008;9:856-69.
23. Stoeckel MC, Weder B, Binkofski F, Choi HJ, Amunts K, Pieperhoff P, Shah NJ, Seitz RJ. Left and right superior parietal lobule in tactile object discrimination. Eur J Neurosci 2004;19:1067-72.
24. Grosbras MH, Leonards U, Lobel E, Poline JB, LeBihan D, Berthoz A. Human cortical networks for new and familiar sequences of saccades. Cereb Cortex 2001;11:936-45.
25. Hüfner K, Stephan T, Glasauer S, Kalla R, Riedel E, Deutschländer A, Dera T, Wiesmann M, Strupp M, Brandt T. Differences in saccade-evoked brain activation patterns with eyes open or eyes closed in complete darkness. Exp Brain Res 2008;186:419-30.
26. Dieterich M, Bauermann T, Best C, Stoeter P, Schlindwein P. Evidence for cortical visual substitution of chronic bilateral vestibular failure (an fMRI study). Brain 2007;130:2108-16.
27. Xu P, Huang R, Wang J, Van Dam NT, Xie T, Dong Z, Chen C, Gu R, Zang YF, He Y, Fan J, Luo YJ. Different topological organization of human brain functional networks with eyes open versus eyes closed. Neuroimage 2014;90:246-55.
28. Josephs KA, Xia R, Mandrekar J, Gunter JL, Senjem ML, Jack CR Jr, Whitwell JL. Modeling trajectories of regional volume loss in progressive supranuclear palsy. Mov Disord

2013;28:1117-24.
29. Boxer AL, Geschwind MD, Belfor N, Gorno-Tempini ML, Schauer GF, Miller BL, Weiner MW, Rosen HJ. Patterns of brain atrophy that differentiate corticobasal degeneration syndrome from progressive supranuclear palsy. Arch Neurol 2006;63:81-6.
30. Cornette L, Dupont P, Rosier A, Sunaert S, Van Hecke P, Michiels J, Mortelmans L, Orban GA. Human brain regions involved in direction discrimination. J Neurophysiol 1998;79:2749-65.
31. Schlack A, Sterbing-D'Angelo SJ, Hartung K, Hoffmann KP, Bremmer F. Multisensory space representations in the macaque ventral intraparietal area. J Neurosci 2005;25:4616-25.
32. Bremmer F, Schlack A, Duhamel JR, Graf W, Fink GR. Space coding in primate posterior parietal cortex. Neuroimage 2001;14:S46-51.
33. Klam F, Graf W. Vestibular signals of posterior parietal cortex neurons during active and passive head movements in macaque monkeys. Ann N Y Acad Sci 2003;1004:271-82.
34. Buckner RL, Andrews-Hanna JR, Schacter DL. The brain's default network: anatomy, function, and relevance to disease. Ann N Y Acad Sci 2008;1124:1-38.
35. Martino J, Gabarrós A, Deus J, Juncadella M, Acebes JJ, Torres A, Pujol J. Intrasurgical mapping of complex motor function in the superior frontal gyrus. Neuroscience 2011;179:131-42.
36. Greicius MD, Krasnow B, Reiss AL, Menon V. Functional connectivity in the resting brain: a network analysis of the default mode hypothesis. Proc Natl Acad Sci U S A 2003;100:253-8.
37. Mantini D, Gerits A, Nelissen K, Durand JB, Joly O, Simone L, Sawamura H, Wardak C, Orban GA, Buckner RL, Vanduffel W. Default mode of brain function in monkeys. J Neurosci 2011;31:12954-62.
38. Raichle ME, MacLeod AM, Snyder AZ, Powers WJ, Gusnard DA, Shulman GL. A default mode of brain function. Proc Natl Acad Sci U S A 2001;98:676-82.
39. Mantini D, Caulo M, Ferretti A, Romani GL, Tartaro A. Noxious somatosensory stimulation affects the default mode of brain function: evidence from functional MR imaging. Radiology 2009;253:797-804.
40. Sohn MH, Albert MV, Jung K, Carter CS, Anderson JR. Anticipation of conflict monitoring in the anterior cingulate cortex and the prefrontal cortex. Proc Natl Acad Sci U S A 2007;104:10330-4.
41. Ursu S, Clark KA, Aizenstein HJ, Stenger VA, Carter CS. Conflict-related activity in the caudal anterior cingulate cortex in the absence of awareness. Biol Psychol 2009;80:279-86.
42. Kawamura K, Naito J. Corticocortical projections to the prefrontal cortex in the rhesus monkey investigated with horseradish peroxidase techniques. Neurosci Res 1984;1:89-103.
43. Klingner CM, Volk GF, Brodoehl S, Witte OW, Guntinas-Lichius O. Disrupted functional connectivity of the default mode network due to acute vestibular deficit. Neuroimage Clin 2014;6:109-14.
44. Zhu C, Li Y, Ju Y, et al. Dizziness handicap and anxiety depression among patients with benign paroxysmal positional vertigo and vestibular migraine. Medicine (Baltimore) 2020;99:e23752.
45. Cousins S, Kaski D, Cutfield N, et al. Predictors of clinical recovery from vestibular neuritis: a prospective study. Ann Clin Transl Neurol 2017;4:340-6.
46. Hong SM, Lee HJ, Lee B, et al. Influence of vestibular disease on psychological distress: a multicenter study. Otolaryngol Head Neck Surg 2013;148:810-4.

Cite this article as: Si L, Cui B, Li Z, Li X, Li K, Ling X, Shen B, Yang X. Concurrent brain structural and functional alterations in patients with chronic unilateral vestibulopathy. Quant Imaging Med Surg 2022;12(6):3115-3125. doi: 10.21037/qims-21-655

